Ultrashort-pulse laser plasmas: Fraction of hot electrons escaping from the target and electron spectra in planar and spherical geometry

Ernst E. Fill
Max-Planck-Institut für Quantenoptik, D-85748 Garching, Germany

(Received 27 August 2004; accepted 22 February 2004; published online 2 May 2005)

Hot electrons generated upon interaction of ultrashort, intense laser pulses with solid targets have many applications in various fields of physics. In this paper a simple theory is developed which allows calculation of the fraction of electrons which escape from the target and the altered electron energy distribution at a distance from the target. The theory is worked out in planar and spherical geometry. It is exact if the electrons are instantaneously generated. In planar geometry all particles eventually return to the target. In spherical geometry, however, a fraction of the electrons are found to escape and, moreover, the electron energy spectrum at large distances approaches an asymptotical one. Two examples of initial electron distributions are treated in detail, viz., an exponential and a Lorentzian distribution. © *2005 American Institute of Physics*. [DOI: 10.1063/1.1891025]

I. INTRODUCTION

The effect of hot-electron generation by interaction of a high-intensity laser pulse with a solid target has received considerable attention in recent years.[1–7] This is because laser-generated ultrashort electron bursts may have a number of applications, such as in laser fusion, x-ray lasers, generation of ion beams, material science, and femtosecond (fs) laser chemistry.

The emission of intense, ultrashort electron bunches from a conductor into a vacuum exhibits interesting features. While the electrons propagate into the vacuum region strong electrostatic self-fields slow them down and eventually pull a great part of them back to the target. At increasing distance from the target fewer and fewer electrons are therefore expected to be observed. In addition, the energy distribution of the electrons is expected to be significantly altered with respect to the original electron spectrum.

In many experiments it is important to know what fraction of the original electrons propagates beyond a certain distance from the target and how the electron spectrum is altered by the self-fields. For example, in irradiating samples it is necessary to determine which kind of radiation—x rays or electrons—dominates the dose received by the specimen: This question arises in investigations for developing optics for fourth-generation light sources, ultrashort-pulse x-ray diffraction experiments, and pumping of x-ray lasers.[8–10]

A complete theoretical assessment of the effects mentioned above is only possible numerically, e.g., by means of particle-in-cell (PIC) simulations. It is shown here, however, that for very short electron pulses the effect of the self-fields can be treated with a relatively simple analytical theory. With laser pulses in the 10 fs range becoming available in more and more laboratories[11] this analytical treatment is gaining increasing relevance to experiments.

In previous work the analytical theory of an infinitely short electron pulse was worked out in planar geometry. With a Lagrangian coordinate for the electrons, the equation of motion together with the Poisson equation was solved, and particle trajectories, electron densities, escape probabilites, and electron spectra were calculated.[12–15]

In spherical geometry the equation of motion together with the Poisson equation cannot be solved analytically. However, it will be shown that energy considerations allow one to calculate the fraction of electrons propagating beyond a certain distance from the target and derive the electron spectrum. The result of these calculations shows that the spherical case is quantitatively but also *qualitatively* different from the planar case. The spherical geometry relations transform to those derived for planar geometry if the initial radius of the electrons is made infinitely large.

The paper is organized as follows: Sec. II gives a short account of the theory in planar geometry. In Sec. III the theory is worked out in spherical geometry. In Sec. IV simple analytical expressions are derived for two specific electron energy distributions. In Sec. V the theory is applied to experimental situations.

II. INSTANTANEOUSLY RELEASED ELECTRONS WITH ARBITRARY ENERGY DISTRIBUTION IN PLANAR GEOMETRY

Consider a planar pulse of electrons instantaneously released from a conductor. The total areal density of the electrons is N_a and the coordinate in the direction of electron propagation is denoted by x. A positive surface charge equal to the charge of the electron cloud provides global charge neutrality and makes the field zero in the conductor. Thus, the field is zero in the conductor, sharply rises close to the boundary to become positive at the surface itself, and then slowly decays along the electron cloud to become zero again at the outermost particle.

If electrons are instantaneously released they cannot overtake each other and thus can be described by means of a Lagrangian coordinate ξ which may be defined as

$$\xi(U) = \int_U^\infty f(U')dU'. \tag{1}$$

Here U is the energy of the electrons and $f(U)dU$ is their normalized energy distribution. $\xi(U)$ ranges from 0 to 1 and gives the fraction of the electrons with an energy $\geqslant U$.

The higher the energy of the electrons the further they will have propagated away from the conductor. Thus, the Lagrangian coordinate ξ denotes the fraction of electrons that have propagated further out from the target. If the total areal density of electrons released from the target is given by N_a, then for an electron population with coordinate ξ the areal density of electrons further out from the target is given by ξN_a. The Poisson equation yields for the electric field E in the vacuum region

$$E = 4\pi e \xi N_a, \tag{2}$$

where e is the elementary electric charge.

It follows from Eq. (2) that electrons with Lagrangian coordinate ξ experience a constant decelerating force given by $-4\pi e^2 \xi N_a$ and thus at a distance x from target the loss of kinetic energy of that electron population is given by

$$\Delta U = 4\pi e^2 \xi N_a x. \tag{3}$$

A. Fraction of electrons propagating beyond a certain distance from the target

In Refs. 14 and 15 the equation of motion of the electrons is solved and the maximum distance is calculated by requiring the velocity to be zero. However, the distance a particular electron population ξ can separate from the target can simply be calculated by equating the energy loss to the original energy $U(\xi)$. This yields, for the maximum distance by which an electron with Lagrangian coordinate ξ moves away from the target,

$$x = U(\xi)/4\pi e^2 \xi N_a. \tag{4}$$

Here $U(\xi)$ is the inverse of $\xi(U)$ as defined in Eq. (1). For any electron energy distribution, Eq. (4) allows one to calculate the fraction of electrons propagating beyond a distance x from the target. In general, this must be done by numerically integrating Eq. (1) and inverting it. However, simple algebraic relations are obtained for electron energy distributions $f(U)$ which can be integrated and the integral function of which can be analytically inverted. This is exemplified in the last part of the paper for an exponential and a Lorentzian distribution.

B. Electron energy spectrum at a distance from the target in planar geometry

The Lagrangian coordinate description allows calculation of the energy spectrum of the electrons at any distance from the target: Since electrons with Lagrangian coordinate ξ lose a kinetic energy $\Delta U = 4\pi e^2 x \xi N_a$ after they have propagated a distance x away from the target, the remaining energy of these electrons is given by

$$U = U_0 - 4\pi e^2 x \xi N_a, \tag{5}$$

where U_0 is the original energy of the electrons. Differentiating with respect to ξ, one obtains

$$\frac{\partial U}{\partial \xi} = \frac{\partial U_0}{\partial \xi} - 4\pi e^2 x N_a. \tag{6}$$

Realizing from Eq. (1) that the fraction of electrons in an energy interval dU is given by $-(\partial\xi/\partial U)dU$, one obtains the energy spectrum of the electrons by varying ξ from 0 to 1 and plotting $-\partial\xi/\partial U = -1/(\partial U/\partial\xi)$ vs U from Eq. (5). Again, the equations become simple for integrable and invertable electron energy distributions (see Sec. IV).

III. ELECTRON ESCAPE AND ELECTRON SPECTRUM IN SPHERICAL GEOMETRY

Consider hot electrons escaping from a target in the form of a sphere with radius r_0. In spherical geometry the Poisson equation (the first Maxwell equation) reads

$$\frac{\partial E}{\partial r} + \frac{2}{r}E = 4\pi n_e e, \tag{7}$$

where r is the radial coordinate, n_e is the local electron density, and E is the electric field. Integrating Eq. (7) with the boundary condition that the field be zero at infinity yields for the field at position r

$$E = \frac{4\pi e}{r^2}\int_r^\infty r'^2 n_e dr'. \tag{8}$$

This equation can, of course, be directly derived from Gauss's law in spherical coordinates. It states that for a centrosymmetric system the field at any position r depends only on the total charge outside r and not on the radial distribution of this charge. Again the Lagrangian coordinate ξ is defined as the fraction of electrons found beyond r,

$$\xi = \frac{4\pi}{N_e}\int_r^\infty n_e r'^2 dr' \tag{9}$$

where N_e, the total number of electrons, is given by

$$N_e = 4\pi \int_{r_0}^\infty n_e r'^2 dr'. \tag{10}$$

Using Eq. (8) the field can now be expressed by the Lagrangian coordinate as

$$E(r) = e\xi N_e/r^2. \tag{11}$$

The energy loss of electrons with Lagrangian coordinate ξ is given by

$$\Delta U = e^2 \xi N_e \int_{r_0}^r \frac{dr'}{r'^2}, \tag{12}$$

which can be integrated to yield

$$\Delta U = e^2 \xi N_e (1/r_0 - 1/r). \tag{13}$$

Thus, an equation analogous to Eq. (5) for the fraction of electrons propagating beyond a radius r can be written down

by equating the energy loss to the original energy $U(\xi)$, resulting in

$$1/r = 1/r_0 - U(\xi)/(e^2 \xi N_e). \tag{14}$$

To relate the expressions for planar and spherical geometry to each other, the total number of electrons N_e is expressed by the areal density N_a of electrons at the emitting sphere by

$$N_e = 4\pi r_0^2 N_a. \tag{15}$$

Equation (14) now reads

$$1/r = 1/r_0 - U(\xi)/(4\pi e^2 \xi r_0^2 N_a). \tag{16}$$

This equation allows one to calculate the fraction of electrons separating a certain distance from the target. Realizing that the distance from the spherical target is given by $x=r-r_0$, one may write Eq. (16) as

$$x r_0/(r_0 + x) = U(\xi)/4\pi e^2 \xi N_a. \tag{17}$$

This form of the equation shows that in the limit that the radius of the emitting sphere becomes infinite, Eq. (17) transforms into the equation for the planar case: For $r_0 \to \infty$, the term $r_0/(r_0+x) \to 1$ and Eq. (17) transforms into Eq. (4).

The spectrum of the electrons at any distance x from the target can be calculated by analogy with the planar geometry. Inserting (15) in (13) the energy loss is written as $\Delta U = 4\pi e^2 \xi N_a x r_0/(r_0+x)$ and the spectrum is again obtained by varying ξ and plotting $-(\partial U/\partial \xi)^{-1}$ vs U with

$$U = U_0 - 4\pi e^2 \xi N_a x r_0/(r_0 + x) \tag{18}$$

and

$$\frac{\partial U}{\partial \xi} = \frac{\partial U_0}{\partial \xi} - 4\pi e^2 \xi N_a x r_0/(r_0 + x). \tag{19}$$

Again, if the radius of the emitting sphere becomes infinite, i.e., $r_0 \to \infty$, then the equations transform to Eqs. (5) and (6) of the planar case.

A remarkable difference in the spherical and the planar cases arises if the distance from the target goes to infinity: In the planar case all electrons eventually come back to the target. This follows from Eq. (3), which shows that at an infinite distance from the target the energy loss becomes infinite. In spherical geometry, however, for $x \to \infty$ part of the electrons escape from the target. From Eq. (17), with $x \to \infty$, one obtains for their fraction ξ_∞ the transcendental equation

$$U(\xi_\infty)/(4\pi e^2 \xi_\infty r_0 N_a) = 1. \tag{20}$$

Furthermore, in the planar case the energy spectrum of the electrons continuously changes as x is increased. In the spherical case, for $x \to \infty$ the factor $x r_0/(r_0+x)$ in Eqs. (18) and (19) goes to r_0 and thus at a large enough distance from target the spectrum does not change any more. The asymptotic spectrum is calculated by varying ξ and plotting $-(\partial U/\partial \xi)^{-1}$ vs U with $U = U_0 - 4\pi e^2 \xi N_a r_0$ and $\partial U/\partial \xi = (\partial U_0/\partial \xi) - 4\pi e^2 N_a r_0$.

IV. SPECIFIC ELECTRON ENERGY DISTRIBUTIONS

In the following the formalism outlined above is applied to two specific electron energy distributions, viz., an exponential and a shifted Lorentzian distribution. These distribution functions can be integrated and the integral function can be inverted, resulting in analytical formulae for the above expressions.

The exponential distribution is the most common one encountered in experimental work and derived in PIC simulations. In experiments with solid targets it is found that the electron distribution can be described by an effective temperature, which for laser intensities in the range of 10^{18}–10^{19} W/cm^2 is 0.2–1 MeV.[6]

A Lorentzian distribution is useful in approximating distributions observed after the electrons have propagated through a conducting solid. It can be further used to approximate quasimonoenergetic distributions observed in recent experiments (see Sec. V).

To simplify the expressions, dimensionless units are used in the following by introducing a normalizing distance $x_n = (4\pi r_e N_a)^{-1}$. Here $r_e = e^2/mc^2 = 2.82 \times 10^{-13}$ cm is the classical electron radius. As an example, at a typical experimental areal density of $N_a = 10^{15}$ cm^{-2} one has $x_n = 2.8$ μm. The dimensionless distances and radii will be denoted by $X = x/x_n$ and $R = r/x_n$.

A. Exponential electron energy distribution

The normalized exponential distribution reads $f(U) = 1/kT_e \exp(-U/kT_e)$, where kT_e is the electron temperature. Inserting this in Eq. (1) and integrating yields

$$\xi(U) = \exp(-U/kT_e), \tag{21a}$$

which is inverted to

$$U(\xi) = -kT_e \ln \xi. \tag{21b}$$

Inserting Eq. (21b) in Eq. (4), one obtains for the normalized maximum distance in planar geometry

$$X = -\frac{kT_e}{mc^2}\frac{\ln \xi}{\xi}. \tag{22}$$

For $X \to \infty$ it is seen that ξ goes to zero, indicating that no electrons escape completely from the target.

In spherical geometry, with Eq. (21b) inserted in Eq. (16), the normalized maximum distance X is found to be given by

$$\frac{1}{R_0 + X} = \frac{1}{R_0} + \frac{1}{R_0^2}\frac{kT_e}{mc^2}\frac{\ln \xi}{\xi}. \tag{23}$$

Using this form of the equation, one can readily appreciate that at $X \to \infty$ the value of ξ does not become zero. A fraction ξ_∞ of the electrons escape from the target, a given by

$$\frac{\ln \xi_\infty}{\xi_\infty} = -\frac{mc^2}{kT_e} R_0. \tag{24}$$

Figure 1 shows transmitted electron fractions vs normalized distance for several electron temperatures comparing planar and spherical geometry. It is seen how in planar geometry the

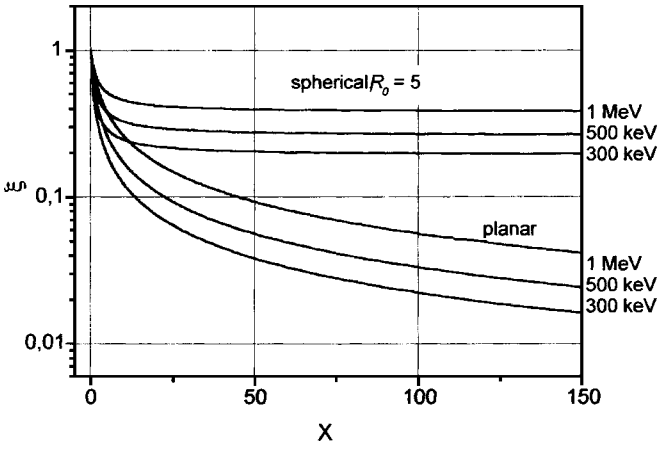

FIG. 1. Transmitted electron fractions as a function of normalized distance from the target in planar and spherical geometry. Dimensionless target radius $R_0=5$. The initial electron energy distributions are exponential with temperatures $kT_e=300$ keV, 500 keV, and 1 MeV. For an areal electron density $N_a=10^{15}$ cm^{-2}, $X=100$ corresponds to a distance of 280 μm from target and $R_0=5$ corresponds to radius of the spherical emitter of 14 μm.

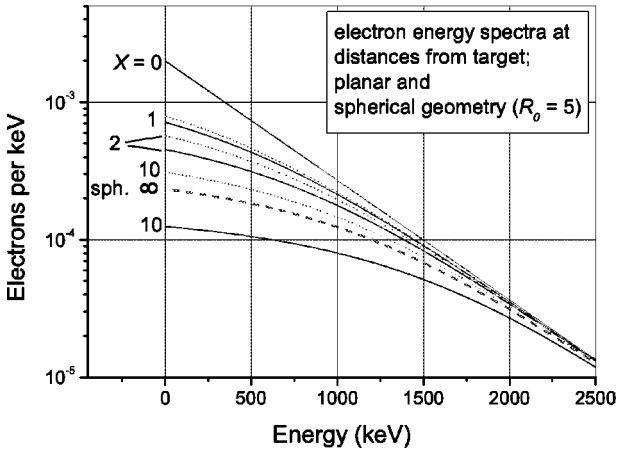

FIG. 2. Electron energy spectra at three distances from the target (dimensionless, $X=0$, 1, 2, 10). Planar and spherical geometry with dimensionless target radius $R_0=5$. The initial electron energy distribution (at $X=0$) is exponential with a temperature of 500 keV. Spherical spectra are drawn dotted. The asymptotic spectrum for spherical geometry is also shown (dashed line termed sph. ∞).

fraction of electrons continuosly decreases, whereas in spherical geometry it approaches a constant value.

To calculate the electron spectrum in planar geometry, Eq. (21b) is inserted in Eqs. (5) and (6). The equations for the spectrum become

$$U = -kT_e \ln \xi - mc^2 \xi X \tag{25a}$$

and

$$-\frac{\partial U}{\partial \xi} = kT_e/\xi + mc^2 X. \tag{25b}$$

In the spherical case Eq. (21b) is inserted in Eqs. (18) and (19), yielding the equations for the spectrum

$$U = -kT_e \ln \xi - mc^2 \xi X \frac{R_0}{R_0 + X}, \tag{26a}$$

$$-\frac{\partial U}{\partial \xi} = kT_e/\xi + mc^2 X \frac{R_0}{R_0 + X}. \tag{26b}$$

For $X \to \infty$ the spectrum approaches an asymptotical one given by

$$U = -kT_e \ln \xi - mc^2 \xi R_0, \tag{27a}$$

$$-\frac{\partial U}{\partial \xi} = kT_e/\xi + mc^2 R_0. \tag{27b}$$

Figure 2 shows electron energy spectra at various distances for an original exponential distribution with $kT_e=500$ keV. The spectrum for the planar case is seen to change gradually with distance, whereas the spectrum for spherical geometry approaches an asymptotic form.

B. Shifted Lorentzian distribution

This distribution is symmetric around its maximum. By making the width arbitrarily small, a monoenergetic distribution may be approximated. Generation of quasimonoenergetic electrons was predicted by simulations[16] and recently observed in experiments.[17–19] After some straightforward calculation the normalized form of the shifted Lorentzian is found to be

$$f(U) = \frac{C}{1 + 4\dfrac{(U - U_c)^2}{w^2}} \tag{28}$$

with the normalization constant

$$C = 4/(\pi w B), \tag{29}$$

where $B=1+(2/\pi)\tan^{-1}(2U_c/w)$. In these equations U_c is the energy of the maximum and w is the full width at half maximum (FWHM). Inserting Eq. (28) into Eq. (1) and integrating results in the relation

$$\xi(U) = \frac{1}{B}\left[1 - \frac{2}{\pi}\tan^{-1}\frac{2(U - U_c)}{w}\right], \tag{30}$$

which can be inverted to yield

$$U(\xi) = U_c + \frac{w}{2}\tan\left[\frac{\pi}{2}(1 - B\xi)\right] \tag{31}$$

and

$$\frac{\partial U}{\partial \xi} = -\frac{w\pi}{4}\frac{B}{\cos^2\left[\dfrac{\pi}{2}(1 - B\xi)\right]}. \tag{32}$$

Using Eq. (31) in Eq. (4) the electron escape fraction for the planar case is readily obtained as

$$X = \left\{U_c + \frac{w}{2}\tan\left[\frac{\pi}{2}(1 - B\xi)\right]\right\}/mc^2\xi. \tag{33}$$

To obtain the spectrum for the planar case, expressions (31) and (32) are inserted in Eqs. (5) and (6), yielding

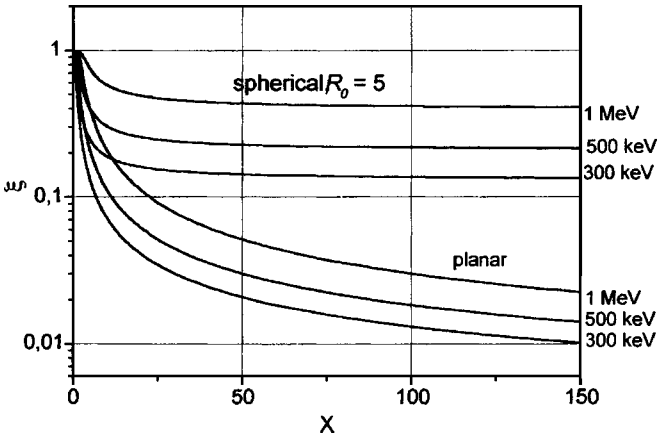

FIG. 3. Transmitted electron fractions as a function of normalized distance from the target in planar and spherical geometry. Dimensionless target radius $R_0=5$. Initial electron energy distributions are shifted Lorentzians with maxima at 300 keV, 500 keV, and 1 MeV and full widths at half maximum (FWHM) of 30 keV, 50 keV, and 100 keV, respectively.

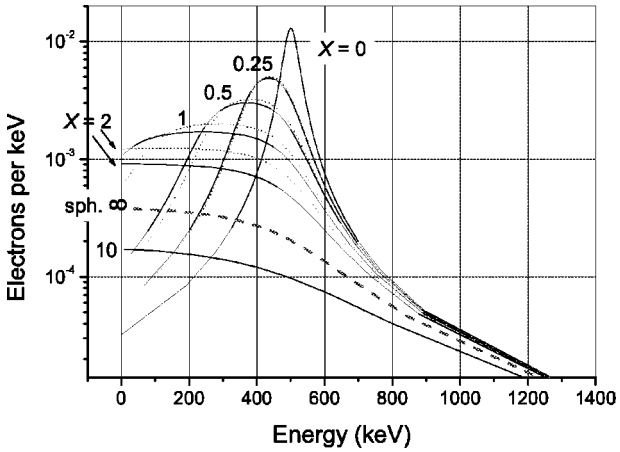

FIG. 4. Electron energy spectra at dimensionless distances $X=0$, 0.25, 0.5, 2, 10 from the target. Planar and spherical geometry with dimensionless target radius $R_0=5$. Spherical geometry spectra are drawn dotted. Spectrum for $X=10$ is only shown for planar geometry. The initial electron energy distribution (at $X=10$) is a shifted Lorentzian with an energy of 500 keV at its peak and a FWHM of 50 keV. The assymptotic spectrum for spherical geometry is also shown (dashed line termed sph. ∞).

$$U = U_c + \frac{w}{2}\tan\left[\frac{\pi}{2}(1 - B\xi)\right] - mc^2 X\xi \tag{34}$$

and

$$\frac{\partial U}{\partial \xi} = -\frac{w\pi}{4}\frac{B}{\cos^2\left[\frac{\pi}{2}(1 - B\xi)\right]}mc^2 X. \tag{35}$$

For spherical geometry, one obtains the formulas for calculating electron escape fractions and electron spectra by inserting Eq. (31) into Eq. (17) and Eqs. (31) and (32) into Eqs. (18) and (19). This yields, for the escape fraction at the normalized distance X,

$$XR_0/(R_0 + X) = \left\{U_c + \frac{w}{2}\tan\left[\frac{\pi}{2}(1 - B\xi)\right]\right\}/\xi mc^2. \tag{36}$$

The equations for the electron spectra are given by

$$U = U_c + \frac{w}{2}\tan\left[\frac{\pi}{2}(1 - B\xi)\right] - mc^2 \xi XR_0/(R_0 + X) \tag{37}$$

and

$$\frac{\partial U}{\partial \xi} = -\frac{w\pi}{4}\frac{B}{\cos^2\left[\frac{\pi}{2}(1 - B\xi)\right]} - mc^2 XR_0/(R_0 + X). \tag{38}$$

The asymptotic forms of these equations, for $X\to\infty$, are obtained by taking the term $XR_0/(R_0+X)$ to be equal to R_0.

Examples of results for originally Lorentzian spectra are given in Fig. 3, showing the fraction of electrons found beyond a normalized distance X from the target. Figure 4 shows the change in the electron spectrum with increasing distance from the target for planar and spherical geometry. The asymptotic spectrum obtained for spherical geometry is also shown in the figure.

V. APPLICATION

Apart from the possibility of calculating electron transmissions and electron distributions, the above theory allows some general conclusions to be made. For example, in an exponential distribution one notes that the number of electrons found beyond a certain distance from the target is not proportional to the total number of electrons released but is reduced in relation to that number. This can be seen by examining Eq. (22). Returning to physical quantities, one may write this equation as $\xi/\ln\xi = -(1/4\pi x N_a r_e)kT_e/mc^2$. The right-hand side is seen to be proportional to $1/N_a$. However, the term $\ln\xi$ in the denominator of the left-hand side makes the dependence of ξ on N_a somewhat weaker This is illustrated in Fig. 5, which gives the areal density of the electrons as a function of the distance from the target for different initial areal densites.

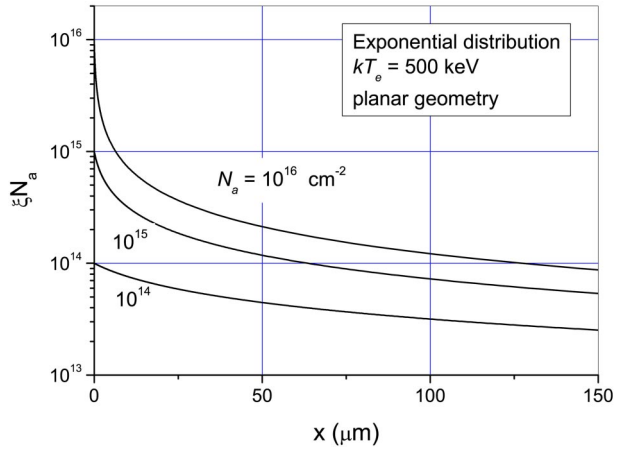

FIG. 5. Areal density of the electrons as a function of the distance from the target for the three total areal densities of $N_a=10^{14}$, 10^{15}, and 10^{16} cm^{-2}. Exponential distribution with $kT_e=500$ keV. The geometry is planar.

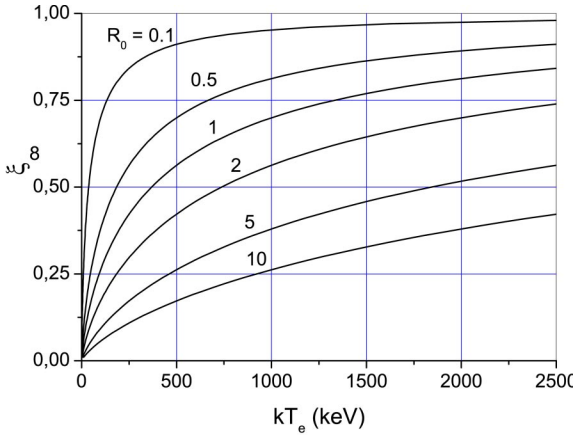

FIG. 6. Fraction of electrons ξ_∞ escaping to infinity in spherical geometry as a function of electron temperature. The dimensionless radius R_0 of the emitting surface is used as a parameter with $R_0=0.1$, 0.5, 1, 2, 5, 10.

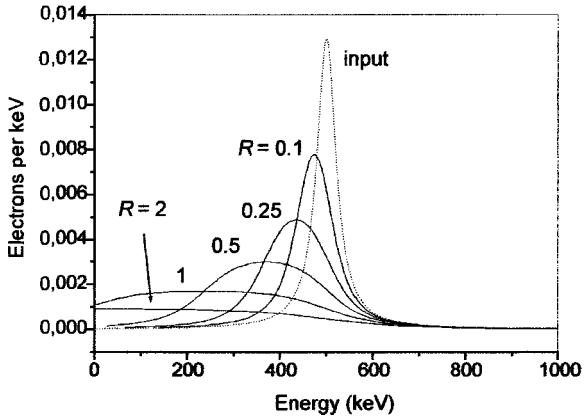

FIG. 7. Asymptotic electron energy spectra of originally Lorentzian distribution in spherical geometry for different dimensionless target radii R_0. The original distribution is drawn dashed (termed "input"). It is a shifted Lorentzian with a peak energy and width of 500 keV and 50 keV, respectively. Asymptotic spectra are shown for dimensionless target radii of 0.1, 0.25, 0.5, 1, and 2.

A most significant result of this theory is the prediction that in spherical geometry a sizable fraction of the electrons escapes to infinity and the possibility to calculate that fraction. The spherical geometry is approached in many experiments since electron beams are usually generated at a small spot and expand at a certain angle. The theory explains why in experiments electrons are seen at all at macroscopic distances from the target. For an exponential electron energy distribution the fraction of electrons escaping from target is given by Eq. (24). As an example, this fraction is displayed in Fig. 6 as a function of electron temperature with the dimensionless radius R_0 as a parameter. The figure shows that for small radii the majority of the electrons escapes from target at electron temperatures exceeding a few hundred keV.

An essential aspect for understanding experimental results is the observation that in spherical geometry the electron spectrum becomes invariant at a large distance from the target. If the target radius is too big, the asymptotic spectrum only vaguely reflects the original spectrum of the source. The influence of target radius on the asymptotic spectrum is illustrated in Fig. 7, which shows asymptotic spectra of an initially Lorentzian distribution as a function of the initial target radius. It is seen that the smaller the target radius the better conserved is the original spectrum.

A possible application of this theory relates to recent experiments in which wakefield-accelerated quasimonoenergetic electron energy distributions were observed.[17–19] In these experiments some 10^9 electrons with energies of around 100 MeV and an energy spread of a few percent are generated. The electron beams are well collimated, with an angular divergence in the region of 10 mrad. The initial diameter of the electron beams is about 25 μm, resulting in an areal density N_a of around 2×10^{14} cm^{-2}.

Applying the theory to these conditions, we note that the apparent radius r_0 of a spherical emitter can be related to the beam divergence ϕ and the initial beam diameter d by the simple relation $r_0=d/\phi$. A beam diameter of 25 μm and a beam divergence of 10 mrad therefore result in an emitter radius of $r_0=2.5$ mm.

A further point of consideration is the fact that the quasimonoenergetic electron population "sits" on a large pedestal of lower energy electrons. The total number of electrons emitted is reported to be about five to ten times that in the monoenergetic bunch. Screening by these electrons can relatively easily be taken into account by reducing the normalization constant C in Eq. (28) by an appropriate screening factor S. Concomitantly, the maximum value of ξ must also be reduced by the same factor. With these modifications the analytical formulae for the Lorentzian energy distribution can still be used and the electrons screening the quasimonoenergetic pulse from the emitter are taken care of.

Figure 8 shows how an originally symmetric narrow electron spectrum is altered after the electrons propagate a certain distance away from the emitter. Quasimonoenergetic ultrarelativistic electrons with a peak energy of 80 MeV and a FWHM of 4 MeV are assumed. The beam divergence is 10 mrad and a screening factor of 10 takes broadly distributed

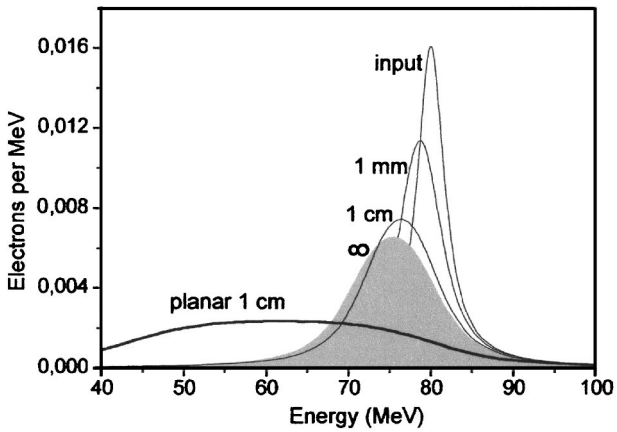

FIG. 8. Electron spectrum of quasimonoenergetic ultrarelativistic electron population after propagating macroscopic distances from the emitter. Distances are indicated in the figure. The spectrum labeled ∞ is the asymptotic spectrum in spherical geometry. The areal electron density is $N_a=2\times10^{14}$ cm^{-2}, the beam divergence 10 mrad. The original spectrum (termed input) peaks at 80 MeV with a FWHM of 4 MeV. A screening factor of 10 is assumed, which takes into account electrons at lower energies.

lower energy electrons into account. It is seen that the original spectrum is broadened and slightly shifted to lower energies. However, after 10 cm of propagation an asymptotic spectrum is already obtained. In planar geometry, however, the change in the spectrum would be severe after a separation of the bunch of only 1 cm from the emitter.

VI. CONCLUSION

The electrostatic fields generated by electron beams themselves severely affect propagation of these beams away from the target. The theory developed in this paper allows calculation of the number of electrons propagating a certain distance away from the target and the change in the electron spectrum to be determined. It is found that in planar geometry these changes are severe. However, in spherical geometry, which may be approached in experiments by an expanding beam, the changes are not so severe, with the spectrum approaching an asymptotic one after a certain distance.

In applying the theory one has to keep in mind the restrictions imposed on it by the approximations made. Note that the theory is exact and fully relativistic for the relevant geometries (planar and spherical) if the electrons are released instantaneously. This condition is fulfilled the better the shorter the pulse generating the electrons is. Furthermore, one has to consider that only electrostatic effects are taken into account by the theory, magnetic field effects being neglected. In most cases, however, the electrostatic effects considered here are expected to dominate. The relative magnitude of the two can be assessed by comparing the electron beam current to the Alfven current $I_A = \beta\gamma 17$ kA. Here β and γ are the particle velocity divided by c and the relativistic mass factor, respectively. With reference to the example in the last section it is seen that magnetic effects are expected to be negligible owing to the high γ factor of the beam electrons.

The possibility of obtaining quasianalytic expressions for the electron transmission and the electron spectrum under a wide variety of experimental conditions and even at ultrahigh energies may make this relatively simple theory useful, e.g., to assess the accuracy and feasibility of PIC simulations.

ACKNOWLEDGMENT

This work was supported in part by the European Communities in the framework of the Euratom-IPP Association.

[1] M. Borghesi, A. J. Mackinnon, A. R. Bell, G. Malka, C. Vickers, O. Willi, J. R. Davies, A. Pukhov, and J. Meyer-ter-Vehn, Phys. Rev. Lett. **83**, 4309 (1999).
[2] J. R. Davies, A. R. Bell, and M. Tatarakis, Phys. Rev. E **59**, 6032 (1999).
[3] D. C. Eder, G. Pretzler, E. Fill, K. Eidmann, and A. Saemann, Appl. Phys. B: Lasers Opt. **70**, 211 (2000).
[4] D. W. Forslund, J. M. Kindel, and K. Lee, Phys. Rev. Lett. **39**, 284 (1977).
[5] P. Gibbon and E. Förster, Plasma Phys. Controlled Fusion **38**, 769 (1996).
[6] G. Malka and J. L. Miquel, Phys. Rev. Lett. **77**, 75 (1996).
[7] L. Gremillet, F. Amiranoff, S. D. Baton, J.-C. Gauthier, M. Koenig, E. Martinolli, F. Pisani, G. Bonnaud, C. Lebourg, C. Rousseaux, C. Toupin, A. Antonicci, D. Batani, A. Bernardinello, T. Hall, D. Scott, P. Norreys, H. Bandulet, and H. Pepin, Phys. Rev. Lett. **83**, 5015 (1999).
[8] E. Fill, D. Eder, K. Eidmann, J. Meyer-ter-Vehn, G. Pretzler, A. Pukhov, and A. Saemann, in *X-ray Lasers 1998*, edited by Y. Kato, H. Takuma, and H. Daido (IoP, Kyoto, 1998), Vol. 159, p. 301.
[9] G. Pretzler, T. Schlegel, E. Fill, and D. C. Eder, Phys. Rev. E **62**, 5618 (2000).
[10] G. Dyer, R. Sheppherd, J. Kuba, E. Fill, A. Wootton, P. Patel, D. Price, and T. Ditmire, J. Mod. Opt. **50**, 2495 (2003).
[11] T. Brabec and F. Krausz, Rev. Mod. Phys. **72**, 545 (2000).
[12] J. W. Poukey and N. Rostoker, Plasma Phys. **13**, 897 (1971).
[13] A. E. Dubinov, Plasma Phys. Rep. **26**, 409 (2000).
[14] E. Fill, Phys. Plasmas **8**, 4613 (2001).
[15] E. Fill, Phys. Rev. E **70**, 036409 (2004).
[16] A. Pukhov and J. Meyer-ter-Vehn, Appl. Phys. B: Lasers Opt. **74**, 355 (2002).
[17] S. P. D. Mangles, C. D. Murphy, Z. Najmudin, A. G. R. Thomas, J. L. Collier, A. E. Dangor, E. J. Divali, P. S. Foster, J. G. Gallacher, C. J. Hooker, D. A. Jaroszynski, A. J. Langley, W. B. Mori, P. A. Norreys, F. S. Tsung, R. Viskup, B. R. Walton, and K. Krushelnik, Nature (London) **431**, 535 (2004).
[18] C. G. R. Geddes, C. Toth, J. van Tilborg, E. Esarey, C. B. Schroeder, D. Bruhwiler, C. Nieter, J. Cary, and W. P. Leemans, Nature (London) **431**, 538 (2004).
[19] J. Faure, Y. Glinec, A. Pukhov, S. Kiselev, S. Gordienko, E. Lefebvre, J.-P. Rousseau, F. Burgy, and V. Malka, Nature (London) **431**, 541 (2004).